THE RADIATIVE HEATING IN UNDEREXPLORED BANDS CAMPAIGNS

BY D. D. TURNER AND E. J. MLAWER

Spectral radiance observations in extremely dry surface locations can be used to reduce the uncertainty in radiative heating and cooling in the mid-to-upper troposphere due to water vapor absorption.

A view of the ARM facility during RHUBC-II, located at 5320 m MSL on Cerro Toco.

Radiative heating drives the earth's atmospheric circulation, propelling an enormous amount of heat energy poleward from the planet's tropical regions. Atmospheric radiative processes are also the primary impetuses for present-day climate change, a consequence of increased abundances of greenhouse gases. Therefore, computer models designed to simulate current or future climate must include an accurate radiation parameterization. Ensuring a suitable level of accuracy for these radiation codes is anchored, as are all scientific advancements, in quality measurements. Programs such as the Atmospheric Radiation Measurement (ARM) program, founded by the U.S. Department of Energy, have been established to improve aspects of climate simulations related to atmospheric radiative transfer by collecting a large volume of high-quality radiation measurements at a number of locations on the earth's surface (Stokes and Schwartz 1994; Ackerman and Stokes 2003). Spectrally resolved radiation measurements, which contain information about the spectroscopic properties of radiatively active atmospheric constituents such as water vapor, have been particularly important in this effort, leading to significant improvements in high-resolution "line-by-line" radiative transfer models (e.g., Turner et al. 2004). These models, in turn, can be used as ▶

foundations for the faster radiative transfer codes employed by general circulation models (GCMs), which are used for climate simulations. ARM-supported researchers have used this measurement-based process to develop the accurate and fast Rapid Radiative Transfer Model (RRTM; Mlawer et al. 1997), which is used to compute radiative fluxes and heating rates in a number of GCMs.

Surface-based spectrally resolved measurements taken in typical terrestrial environments cannot provide validation in all spectral regions of importance to climate. If the atmosphere in a particular spectral band is opaque to radiation in the vertical layer above the instrument because of strong gaseous absorption, the measurement will yield just the Planck function corresponding to the temperature of that layer. That means that no useful spectroscopic information can be obtained from the measurement; this is essentially the same as trying to visually describe what is happening on the other side of a solid brick wall. Opacity in a vertical layer also implies that no radiative heating occurs in that layer in that spectral band, so with respect to our understanding of key radiative processes in the lowest levels of the atmosphere this situation does not create a problem. However, radiative heating at higher levels in the atmosphere, such as the middle troposphere, upper troposphere, and lower stratosphere, can occur in spectral regions that are opaque at the surface but in the column above that layer become "semi-transparent" (i.e., have a nonzero transmittance from this level to the top of the atmosphere) because of smaller amounts of absorbing gases (e.g., water vapor). For these spectral bands, surface spectral measurements in typical conditions offer no value in improving our understanding of the spectroscopic parameters on which radiative transfer calculations at these higher altitudes are based. At sites where the column amount of water vapor is very low, however, these spectral bands become semi-transparent and surface measurements will contain useful information with respect to the spectroscopic parameters in those bands.

The dominant radiative processes in the middle troposphere to lower stratosphere occur in strong water vapor absorption bands, of which there are many throughout the thermal (i.e., longwave) and solar (shortwave) parts of the electromagnetic spectrum. One particularly important absorption band is the "pure rotational" water vapor band, located in the far-infrared (far-IR) part of the spectrum (wavelengths longer than approximately 15 μm). This spectral region contains a large fraction of the thermal energy (i.e., the Planck function) available at terrestrial temperatures, leading to this band being of critical importance in considerations of the energy balance and radiative heating of the planet. Approximately 40% of the outgoing longwave radiation leaving Earth is emitted by water vapor transitions in this band (Harries et al. 2008); this band also provides about 60% of the longwave radiative cooling in the atmosphere, with an even more significant role in the cooling in the mid-to-upper troposphere (Clough et al. 1992). In addition, radiative processes in this band are critical in understanding the radiative balance of the tropical tropopause layer and the transport of air into the stratosphere (Gettelman et al. 2004). However, because of the strength of this water vapor absorption band, it is typically opaque at the surface, which is one of the key factors that have discouraged instrument developers from building spectral instruments that measure in the far-IR. In the past few years, there has been significant progress in this regard with the development of a number of far-IR spectral instruments, opening the door for detailed evaluation of far-IR model calculations should spectral measurements be taken in suitably dry environments.

This paper describes a set of field experiments initiated by the ARM program, the Radiative Heating in Underexplored Bands Campaigns (RHUBC), which have been specifically designed to improve our understanding of the dominant radiative processes in the middle troposphere, upper troposphere, and lower stratosphere. The locations for the RHUBC campaigns have been chosen for their extremely low water vapor loadings in order to greatly reduce the atmospheric opacity that impedes the study of these processes from the surface. RHUBC I was held from February to March 2007 at the ARM Climate Research Facility (ACRF) in Barrow, Alaska [referred to as the North Slope of Alaska (NSA) ACRF], where water vapor

AFFILIATIONS: Turner—University of Wisconsin—Madison, Madison, Wisconsin; Mlawer—Atmospheric and Environmental Research, Inc., Lexington, Massachusetts
CORRESPONDING AUTHOR: Dr. David Turner, University of Wisconsin—Madison, 1225 West Dayton Street, Madison, WI 53706
E-mail: dturner@ssec.wisc.edu

The abstract for this article can be found in this issue, following the table of contents.
DOI:10.1175/2010BAMS2904.1

In final form 18 December 2009

column amounts (PWV) in the winter can be as low as 1.0–1.5 mm. This first campaign was conducted at the same time as a similar experiment called Earth Cooling by Water Vapor Radiation (ECOWAR) was conducted in the Italian Alps (Bhawar et al. 2008). A second campaign, RHUBC II, was held from August to October 2009 at an elevation of 5320 m at a site near the summit of Cerro Toco in the Atacama Desert of Chile; this experiment includes participants from the ECOWAR community. This region is well known for the dryness of its climate and consequently has also been selected by the astronomical community for the deployment of numerous telescopes and instruments. The time period of RHUBC II corresponds to the lowest water vapor loadings of the year, with PWV values approaching 0.2 mm. In effect, the water vapor abundances at this high-altitude Chilean site are similar to those seen in the mid-to-upper troposphere, a rare occurrence for a surface-based location.

Figure 1b shows the transparency of the atmosphere over most of the longwave spectral region for atmospheric profiles with different water vapor amounts: a profile typical of conditions found at the ARM SGP site, with a PWV of 15 mm; a water vapor, temperature, and pressure profile typical of the conditions encountered in RHUBC I (PWV = 1.5 mm); and a water vapor, temperature, and pressure profile during RHUBC II (PWV = 0.2 mm). This plot is shown at a coarse spectral resolution to provide an overview of the longwave atmospheric transparency; the zoomed view in Fig. 1a provides a more spectrally resolved perspective, directly relevant to the RHUBC I and II analyses. The SGP atmosphere is effectively opaque (transmittance equals 0) for most of the far-IR, but the two other profiles have regions of semi-transparency throughout this spectral domain. For the two drier profiles, throughout the far-IR there are regions of higher transmittance values interspersed with lower transmittances (which correlate strongly with radiance values). As a result, far-IR spectral measurements taken under these dry conditions will contain corresponding fluctuations in radiance, which allows information about the strengths and widths of water vapor absorption lines to be determined. Also, measured radiance values in the "microwindows" (i.e.,

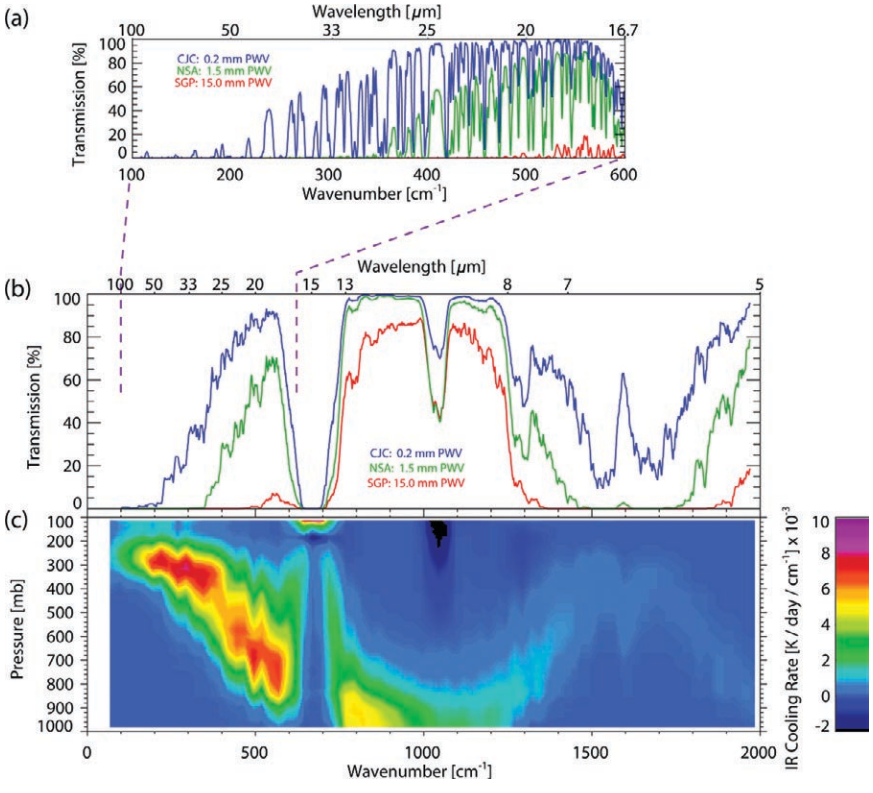

Fig. 1. (a) Atmospheric transmittance at 1-cm^{-1} resolution in the far-infrared for three atmospheres with very different PWV amounts, representative of the ARM Southern Great Plains (SGP) site in north-central Oklahoma, the North Slope of Alaska (NSA) site in Barrow, Alaska, and at the Chajnantor plateau (CJC) in the Atacama Desert in Chile (near the RHUBC II site). Strong absorption by water vapor results in the transmission going to zero, whereas the atmosphere can become semitransparent in "microwindows" between absorption lines. These microwindows become more transparent, and more of them open up at longer wavelengths, as the PWV decreases. (b) The atmospheric transmittance for the same three atmospheres across the majority of the infrared at 25-cm^{-1} resolution. The coarser spectral resolution "blurs" the high-frequency structure seen in (a). (c) After Clough and Iacono (1995), the spectral distribution (at 25-cm^{-1} resolution) of the infrared radiative cooling rates as function of height for a midlatitude summer profile (other profiles shift this figure primarily in the vertical). It should be noted that carbon dioxide has a strong absorption band centered at 667 cm^{-1}, whereas ozone has a strong absorption band centered at 1040 cm^{-1}.

spectral regions between lines, which are associated with the highest transmittance values) are essential in determining the strength of water vapor continuum absorption, a key contributor to the total absorption by water vapor.

The primary objective of these two RHUBC campaigns is to improve the accuracy of line-by-line radiative transfer models in the far-infrared and other spectral regions with strong water vapor absorption bands by reducing the uncertainties of the spectroscopic parameters that are used to model water vapor absorption. Data from the RHUBC campaigns will be used in radiance closure exercises (e.g., Turner et al. 2004; Tobin et al. 1999) wherein atmospheric state observations (profiles of water vapor and temperature) will be used as input into state-of-the-art line-by-line radiative transfer models that are compared against collocated detailed spectral radiance observations. Accurate, calibrated spectral radiance observations are critical; as indicated above, only recently have spectrometers been built that have sensitivity in the far-infrared. Thus, each RHUBC campaign included multiple far-IR spectrometers that use different measurement approaches, thereby allowing a comparison of these critical observations.

Accurate atmospheric state measurements, especially PWV, are also critical for these closure exercises (Revercomb et al. 2003). Because of the extremely low PWV conditions, PWV is retrieved from measurements made near the strong 183-GHz water vapor absorption line, which is much stronger than the 22.2-GHz water vapor line used in the retrieval of PWV at most surface locations (Racette et al. 2005). Commercially available 183-GHz radiometers have only been developed in the past several years, and thus a comparison of these critical observations was also an important component of the RHUBC strategy.

THE WATER VAPOR CONTINUUM

A complete treatment of atmospheric radiative transfer must include the effects of many thousands of absorption lines, each due to a transition between two quantum mechanical states of a gaseous molecule. Line-by-line radiative transfer models have been developed to systematically compute the absorption due to these lines throughout the electromagnetic spectrum. For these calculations, these models employ an assumed spectral line shape and associated spectroscopic parameters, such as line positions, strengths, and spectral widths, provided by line absorption databases such as the High-Resolution Transmission Molecular Absorption (HITRAN) database (Rothman et al. 2009). The accuracy of the radiative transfer calculations then depends on the accuracy of the parameters in the absorption line database, the mathematics of the radiative transfer algorithm, and the adequacy of the assumed line shape in capturing the physics of the transition.

The Lorentz line shape, used in most line-by-line models, is derived based on the simple assumption that the radiating molecule and the colliding molecule undergo an instantaneous interaction at "impact." (Actually, most models use the Voigt line shape, which reduces to a Lorentz line shape at tropospheric pressures.) In reality, the two molecules affect each other over a longer time period, leading to the actual line shape deviating from the idealized Lorentz shape. This deviation is negligible close to the center of the line, where the frequency dependence of the optical depth is determined by the molecules' interaction at long distances—a weak interaction that agrees well with the instantaneous impact approximation. In contrast, the close-range interaction is more complex, resulting in the line shape deviating from the Lorentz profile further from line center.

Line-by-line radiative transfer models typically separate the contribution from a single molecular absorption line into a local line contribution and the "continuum" contribution. The local line contribution is defined as the contribution to the spectral absorption for some fixed distance from line center (typically 25 cm^{-1}), with the contribution at this distance from line center being zero (the red region in Fig. S1). This separation is made primarily to reduce the computational expense of the calculation. Typically, in order to resolve all relevant absorption features, the spectral spacing used in a line-by-line model is 2 to 8 times finer than the half width of the narrowest line for the given atmospheric pressure. Therefore, restricting the spectral range over which any particular absorption line shape is evaluated can greatly reduce the computational burden in a calculation that includes a great number of absorption lines. The ability to cut off the calculation of the line contribution a certain distance from each line center without negatively affecting the calculation accuracy is a result of the slow variation of the line shape with frequency far from the center. Therefore, the contributions of all lines past their cutoff (including, for continuity, the "basement" contribution (Fig. S1) within 25 cm^{-1} of each line center) can be combined into a slowly varying continuum that can be included in a calculation with minimal computational cost. Although the line shape is uncertain that far from the line center, the continuum coefficients can be empirically determined to infer the far-wing properties of the line shape. The continuum can also be constructed to include any deviations from the Lorentz shape within the line cutoff.

For terrestrial atmospheric considerations, the most important example of continuous gaseous absorption is the water vapor continuum. The majority of the absorption

RHUBC I. The first RHUBC campaign was conducted at the NSA site in February through March 2007, which is climatologically the driest period at the Barrow site as well as the period that has the lowest occurrence of optically thick low clouds. For this experiment, three interferometers were deployed that had sensitivity to downwelling radiance in the far-infrared as well as three radiometers that made observations around the 183-GHz water vapor absorption line. Basic details of these instruments are given in Table 1. The NSA ACRF site also has a wide array of other instrumentation important for RHUBC, such as a cloud-sensitive lidar, broadband radiometers, and a radiosonde sounding station. Figure 2 shows the layout of the site during RHUBC I.

The weather during RHUBC I was very favorable with respect to the campaign's objectives, with an extended duration of cold, clear conditions and only a few episodes with liquid water clouds overhead. The RHUBC investigators launched an additional 48 radiosondes during the three-week campaign in clear sky and cirrus conditions, supplementing the twice-daily launches normally performed at the NSA site. The range of PWV observed was 0.95 to 2.5 mm, with a median value of 1.4 mm (Fig. 3). However, a persistent aerosol layer existed for several days, which contributed to the downwelling infrared radiance and complicated the subsequent analysis of the infrared data. Nonetheless, three very important contributions have resulted from RHUBC I.

The first is the demonstration that the three 183-GHz millimeter-wave radiometers agreed very well (within the 1–2-K radiometric uncertainty of the observations) with each other, even though the radiometers used very different measurement designs and calibration approaches (Cimini et al. 2009). Evaluating the accuracy of these observations was a key objective because of the importance of the PWV

occurring in the "atmospheric window" (800–1200 cm^{-1}), a region with significant thermal energy at atmospheric temperatures, is due to water vapor despite the lack of strong water vapor absorption lines nearby. The optical depth of this between-bands continuum has been shown to vary with the square of the water vapor amount, which implies that it is due to the interactions of two water vapor molecules (the "self-continuum"). With a consistent line shape applied to all water vapor lines throughout the electromagnetic spectrum, Clough et al. (1989) used a combination of theory (which predicts a generalized line shape) and semi-empirical fits of a small number of parameters to model the measured self-continuum absorption. This result implied that the water vapor continuum in the atmospheric window was due to the far wings of strong water vapor lines many hundreds of wavenumbers (cm^{-1}) away at the center of the water vapor rotation band in the far-infrared. This work also provided a similar formulation for the foreign (i.e., resulting from the interaction of a water vapor molecule with a molecule of a different type) water vapor continuum, which varies linearly with water vapor abundance and is the dominant source of continuum absorption within water vapor bands (such as in the far-IR). Fitting the measurements of the foreign broadened continuum absorption in this manner can be accomplished if the contributions from water vapor lines are as schematically depicted in Fig. S1: the contributions from the basement term, super-Lorentzian absorption in the near-wing, and sub-Lorentzian far-wing absorption (the gray region in Fig. S1).

The evaluation, and potentially the improvement, of the water vapor continuum model in the far-infrared is a high priority of the RHUBC campaigns.

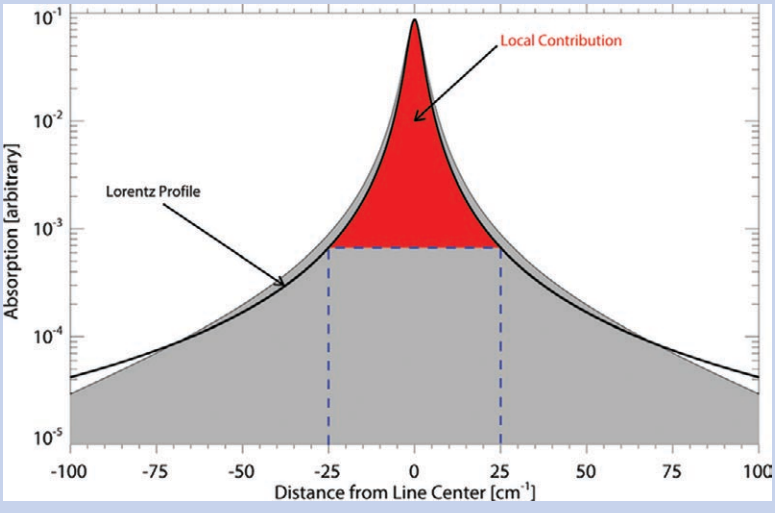

Fig. S1. A hypothetical absorption line showing the local line contribution (red) and the contribution that would be included in the continuum (gray). The basement term is the portion of the absorption under the local line contribution, which is identified here by the blue dashed rectangle. The continuum contribution includes the contribution from the basement, as well as both super- and sub-Lorentzian contributions in the wings of the line.

Table 1. Details of key instruments deployed during RHUBC I.			
Instrument	**Short name**	**Organization/PI/Reference**	**Key details**
Atmospheric Emitted Radiance Interferometer	AERI	ARM/D. Turner/Knuteson et al. 2004a,b	Spectral range 3.3–25 μm, spectral resolution 0.5 cm^{-1}, temporal resolution 20 s, detector is cooled with Stirling cooler
Tropospheric Airborne Fourier Transform Spectrometer	TAFTS	Imperial College/P. Green/Canas et al. 1997	Spectral range 15–125 μm, spectral resolution 0.12 cm^{-1}, temporal resolution 2 s (many spectra are averaged together for ground-based operations), detector cooled with liquid helium
Ground-based scanning radiometer	GSR	University of Colorado/E. Westwater/Cimini et al. 2007, 2009	27-channel submillimeter radiometer with 7 channels around the 183.3-GHz water vapor line, double sideband, calibration uses internal and external loads as well as tip curves, continuous elevation scanning, ~1-min temporal resolution for zenith observations
G-band water vapor radiometer	GVR	ARM/M. Cadeddu/Pazmany 2007	Four-channel submillimeter radiometer at 183.3 GHz, double sideband, calibrated with ambient and hot loads, zenith-only operations, temporal resolution 10 s
Microwave profiler 183	MP-183	Radiometrics/M. Exner/Cimini et al. 2009	Frequency agile microwave radiometer, software tunable from 170 to 183.6 GHz (15 channels used during RHUBC I), continuous elevation scanning and zenith observations, temporal resolution of ~30 s, internal noise diode and ambient target used for calibration
Micropulse lidar	MPL	ARM/C. Flynn/Campbell et al. 2002	Polarization sensitive cloud lidar, 15-m vertical resolution, 30-s temporal resolution, maximum range 60 km
Vaisala RS-92 radiosondes	Sonde	ARM/B. Lesht/Miloshevich 2009	Typically launched twice a day by ACRF site; during RHUBC I the investigators launched additional 48 sondes during clear-sky periods

retrievals from these instruments for the subsequent analysis.

The second important contribution was the refinement of the spectral width of the 183.3-GHz water vapor line (Payne et al. 2008). The accuracy of the strength of this water vapor line is better than 1% (Clough et al. 1973), but the width is also important for the accurate retrieval of PWV from multichannel 183-GHz radiometers.

The third contribution concerned the evaluation of the accuracy of the Line-by-Line Radiative Transfer Model (LBLRTM; Clough et al. 1992) in the 16–25-μm band (Delamere et al. 2010) using pristine (i.e., aerosol-free) clear-sky cases. In this analysis, the PWV retrieved from a 183-GHz radiometer is used to scale the observed radiosonde humidity profile; scaling greatly reduces the uncertainty in the radiosonde humidity profile and mitigates any diurnal bias in the radiosonde observations (Turner et al. 2003; Cady-Pereira et al. 2008). It should be noted that the nighttime water vapor profile measurements (i.e., when the sun is below the horizon) made by the Vaisala RS-92, the type of radiosonde used in both RHUBC experiments, agree very well with chilled mirror hygrometers and have little bias (Miloshevich et al. 2009). The PWV-scaled humidity profiles are then input into the LBLRTM, which computes monochromatic radiance spectra that are convolved with the appropriate instrument function to mimic the Atmospheric Emitted Radiance Interferometer (AERI)-ER observations. These spectral differences between the observations and calculations were then used to improve the spectral widths of many of the strong water vapor lines in this spectral region as well as the foreign water vapor continuum. The impact of the RHUBC I data on the differences between LBLRTM calculations and AERI-ER observations is shown in Fig. 4, with the

updated model having significantly better smaller residuals (both mean and standard deviation) relative to the AERI. These spectroscopic improvements will impact the calculation of mid-to-upper tropospheric longwave cooling rates across the globe in the far-IR (Delamere et al. 2010).

RHUBC I was very successful; however, because of the amount of PWV experienced at the site, the far-infrared was only semi-transparent out to approximately 27 μm. The strongest radiative cooling occurs at even longer wavelengths (30–50 μm) at the lower water vapor abundances in the middle-to-upper troposphere (Clough et al. 1992). Furthermore, RHUBC I concentrated on the far-infrared, but there are near-infrared water vapor absorption bands that contribute to the radiative heating in the mid-to-upper troposphere through their strong absorption of solar radiation. The water vapor absorption parameters in these bands also have significant uncertainties due to the lack of validation with spectral observations. This provided a strong motivation to organize a second RHUBC experiment at a site with even lower water vapor amounts and where the sun rose high in the sky.

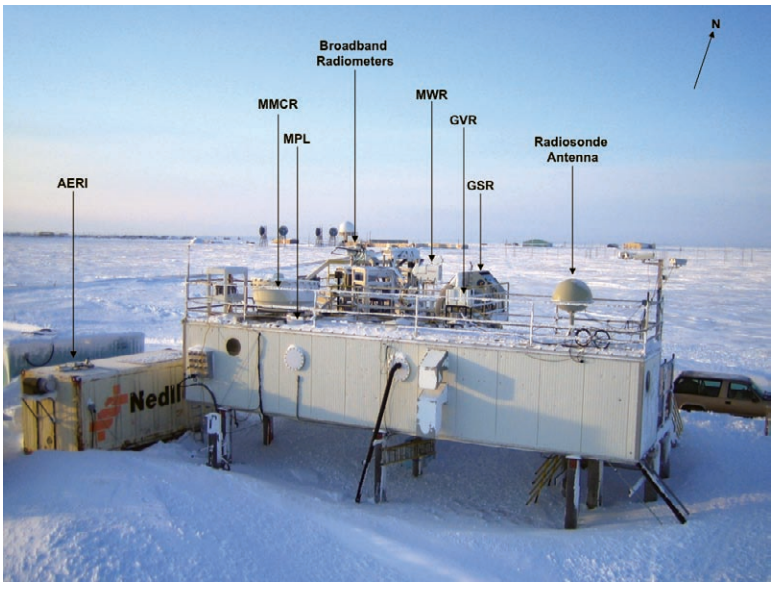

Fig. 2. The NSA ACRF site during RHUBC I, showing the locations of most of the instruments used for the campaign. The Tropospheric Airborne Fourier Transform Spectrometer (TAFTS) and MP-183 were located in the guest user facility just to the east of this facility. The facility in the background of the image is a Distant Early Warning (DEW) line radar station.

RHUBC II. The need to find a site with significantly lower PWV than the NSA ACRF site, a large fraction of clear skies, and periods with solar elevation angles above 30° placed a fairly significant constraint on where the campaign could be conducted. The Atacama Desert in the Andes Mountains of Chile is one of the driest locations of the world (Rutllant Costa 1977) because of the region being in the rain shadow between mountain ranges; the Walker circulation, which causes air to descend upon the Atacama; and the cold ocean water off the coast of Chile, which results in a coastal inversion layer. Furthermore, the Atacama experiences few cloudy periods relative to other locations. Because of the extremely low PWV amounts and number and duration of clear-sky events, the Atacama Desert is the home of numerous astronomical telescope facilities, many of which operate in the sub-millimeter portion of the spectrum, which is only semi-transparent in very dry locations due to strong absorption by water vapor. Many of these facilities in this region have been operational for over a decade.

A location at 5320 m above mean sea level on the mountain Cerro Toco beside the Chajnantor plateau in northern Chile was selected as the site for RHBUC II (Fig. 5). This site is located next to several astronomical facilities, including the Atacama Large Millimeter Array (ALMA) facility and the Atacama Cosmology Telescope (ACT). The annual range of PWV for this region is approximately 0.1–5.0 mm; however, the

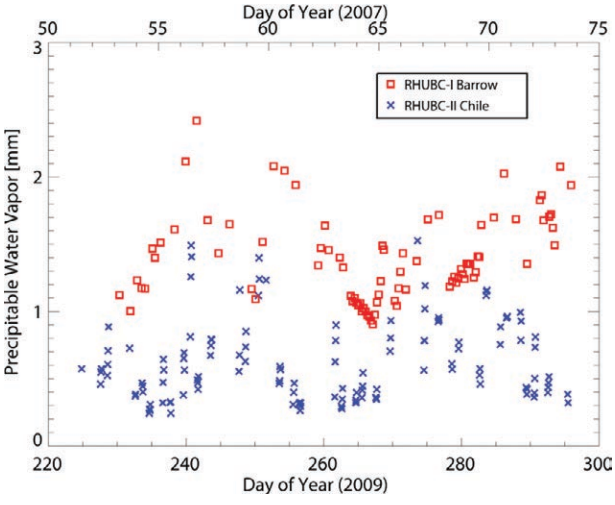

Fig. 3. The PWV observed by radiosondes during RHUBC I and RHUBC II.

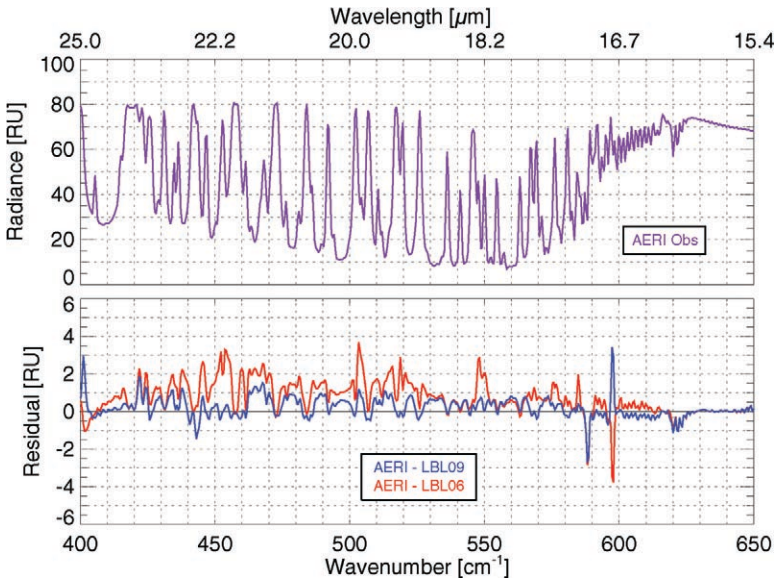

Fig. 4. The mean downwelling radiance observed by the AERI-ER during RHUBC-I (top panel), and the mean observed minus calculated residuals (bottom panel) for two different versions of the LBLRTM during the RHUBC-I period. The LBL06 was the state of the model just prior to RHUBC-I, and LBL09 is the current model that was improved using RHUBC data. The mean (standard deviation) of the radiance residuals in this spectral band are 0.75 (0.89) RU and 0.23 (0.55) RU for the LBL06 and LBL09, respectively; RU = 1 mW / (m² sr cm⁻¹).

PWV distribution is much narrower and is driest during late winter/early spring, with the median PWV of this period being approximately 0.5 mm. Thus, the campaign was conducted in August–October 2009, where the PWV ranged from 0.2 to 1.5 mm (Fig. 3). At the lowest PWV values achieved during RHUBC II (on the order of 0.2 mm), the far-infrared was semi-transparent, thereby allowing the water vapor absorption to be evaluated out to nearly 45 μm.

The ARM program deployed a large suite of instruments in a (sic) Self-Kontained Instrument Platform (SKIP) for RHUBC II. This facility provided shelters for the instruments and manpower, as well as diesel generator power and computing infrastructure. Many ARM instruments that were deployed during RHUBC I were also deployed during the second campaign in Chile. In addition, four additional interferometers and a scanning microwave profiler from collaborating agencies were deployed. Two of these interferometers provided spectrally resolved radiance observations in the far-infrared (out to 100 μm), one provided spectrally resolved radiance observations of the direct solar radiance from 1 to 5 μm, and the last provided spectrally resolved observations in the submillimeter spectral region (300 GHz to 3 THz). Thus, RHUBC II made high-spectral-resolution observations across almost the entire electromagnetic spectrum, from 1 to 1000 μm. A full list of instruments deployed during RHUBC II is listed in Table 2.

During this three-month period, the climatology suggested that the sky would be cloud-free approximately 80% of the time; however, several strong weather events conspired to reduce the amount of clear sky to approximately 70%. The site is close to the Tropic of Capricorn and thus the sun rose high into the sky every day, allowing the attenuation due to water vapor in the near-infrared bands to be studied in addition to the emission by water vapor

Fig. 5. The location of the RHUBC II field site on Cerro Toco in the Atacama Desert, which is located in northern Chile (inset). The location of the Atacama Cosmology Telescope (ACT) astronomical facility is also shown.

in the far-infrared bands. The zenith transmission in the near-infrared is shown in Fig. 6. Note that most of the water vapor absorption bands in the 1–5-μm region are semi-transparent at the low PWV amount expected for the RHUBC II campaign. Data were collected by the Absolute Solar Transmittance Interferometer (ASTI; Table 2) over a range of solar elevations, thereby providing a larger dynamic range of conditions to use in the evaluation of water vapor spectroscopy in the near-infrared.

The RHUBC II experiment provided opportunities to improve radiative transfer models in spectral regions that are important for remote sensing but are less important from a climate point of view. As indicated above, the astronomical facilities in the Atacama use the submillimeter region of the spectrum to view the heavens (Fig. 7); however, their analysis needs to account for the attenuation in these bands due to fluctuating water vapor. Furthermore, the submillimeter offers a powerful way to quantify the ice water path of cirrus clouds from space (Evans et al. 1999), but this approach requires that the clear-sky absorption model is accurate. Data collected by the Smithsonian Astrophysical Observatory (SAO) Fourier Transform Spectrometer (FTS) will be used to evaluate radiative transfer models in this spectral region, which may lead to improvements in the spectral line parameters and/or the water vapor continuum at these wavelengths. The SAO FTS data will also provide an additional validation for recent

Table 2. Details of key instruments deployed during RHUBC II.

Instrument	Short name	Organization/PI/Reference	Key details
Atmospheric Emitted Radiance Interferometer	AERI	ARM/D. Turner/Knuteson et al. 2004a,b	Spectral range 3.3–25 μm, spectral resolution 0.5 cm^{-1}, temporal resolution 7 min, detector is cooled with Stirling cooler, views of zenith and 60° off-zenith radiance
Far-Infrared Spectroscopy of the Troposphere	FIRST	NASA Langley Research Center/M. Mlynczak/Mlynczak et al. 2006	Spectral range 6.3–100 μm, spectral resolution 0.6 cm^{-1}, temporal resolution 10 min, detector is cooled with liquid helium
Radiation Explorer in the Far-Infrared–Prototype for Applications and Development	REFIR–PAD	Istituto di Fisica Applicata–CNR, Italy/L. Palchetti/Palchetti et al. 2005, 2008	Spectral range 7–100 μm, spectral resolution 0.5 cm^{-1}, temporal resolution 15 min, uncooled pyroelectric detector
Absolute Solar Transmittance Interferometer	ASTI	University of Denver/T. Hawat/ Hawat et al. 2002	Spectral range 1–5 μm, spectral resolution 0.6 cm^{-1}, temporal resolution 5 min, detector is cooled with liquid nitrogen, calibration is performed using reference tungsten lamp, solar tracking
Smithsonian Astrophysical Observatory submillimeter FTS	SAO-FTS	Smithsonian Astronomical Observatory/S. Paine/Paine et al. 2000	Spectral range 0.3–3.5 THz (10–116 cm^{-1}), spectral resolution 3 GHz, temporal resolution 10 min, detector cooled with liquid helium
Microwave profiler 183	MP-183	ARM/M. Cadeddu/Cimini et al. 2009	Same as for RHUBC I
Humidity and Temperature Profiler	HATPRO	Univ. Cologne/S. Crewell/Rose et al. 2005	14-channel microwave radiometer (7 channels between 22.2 and 31 GHz, 7 channels between 51 and 58 GHz), temporal resolution 1 s, 3D scanning, noise diodes and internal target used for calibration
Micropulse lidar	MPL	ARM/R. Coulter/Campbell et al. 2002	Same as RHUBC I
Vaisala RS-92 radiosondes	Sonde	ARM/D. Holdridge/Miloshevich et al. 2009	3–5 launched per operations day during RHUBC II

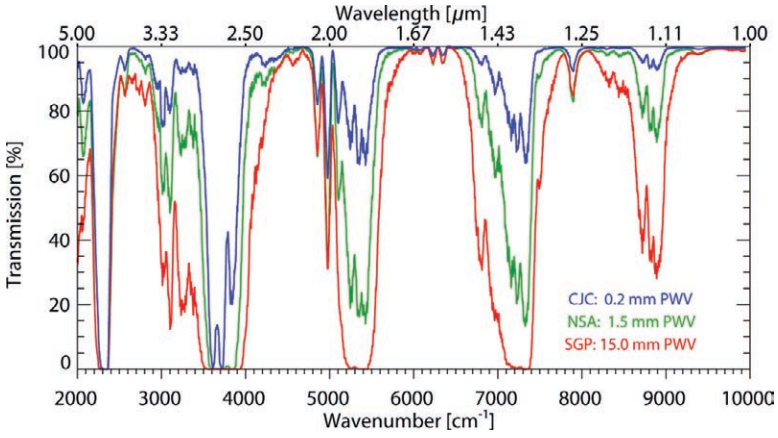

Fig. 6. The zenith transmission in the near-infrared portion of the spectrum for the three atmospheres used in Fig. 1; the spectral resolution is 50 cm^{-1}. The strong absorption band at 2325 cm^{-1} is due to absorption by carbon dioxide; the remaining strong absorption bands shown here are due to water vapor.

analyses on the water vapor continuum absorption models at 150 GHz (Turner et al. 2009; V. Payne et al. 2010, manuscript submitted to *IEEE Trans. Geosci. Remote Sens.*). Additionally, the low surface pressure conditions will allow the spectroscopy of the 60-GHz oxygen absorption complex, which is used to passively profile temperature in the atmosphere (e.g., Crewell and Löhnert 2007), to be further evaluated and potentially improved.

RHUBC II presented many logistical challenges. The site is isolated, requiring diesel generators for power; there were many problems at the beginning of the experiment until the generators were modified to run at the cold, low-oxygen conditions at the site. The scientific and operations staff were only at the Cerro Toco site during operational periods and stayed overnight in a nearby village at an altitude of 2400 m. An operations day had the staff arriving at the Cerro Toco site early in the morning and setting up instruments that were not running continuously [e.g., the Far-Infrared Spectroscopy of the Troposphere (FIRST), Radiation Explorer in the Far Infrared (REFIR), and ASTI]. Data were typically collected until just after local noon, after which the instruments were stored and the site secured. This sampling strategy had three advantages: (i) it captured the early morning period, which climatologically has the lowest amount of PWV over the diurnal cycle; (ii) the wind speeds are the lowest during the morning, thereby minimizing any dust mobilization/advection events, as well as operator fatigue, and (iii) the ASTI experienced the full range of solar elevations. During this operations period, radiosondes were launched every 75–90 minutes, and several instruments required manual interaction for calibration and operation purposes. Reduced oxygen amounts, a consequence of the low surface air pressure at Cerro Toco (~530 mb), made physical activity challenging. Oxygen concentrators were used to enhance the supply of oxygen in several of the SKIP containers, and portable oxygen cylinders were used when needed by most of the on-site staff. To help mitigate the potential altitude issues, and in particular the fatigue associated with working at high altitude, operations typically occurred two days out of every three.

FUTURE. The primary objective of RHUBC I and II is to improve the clear-sky spectroscopy of water vapor in the strong water vapor absorption bands in spectral regions that are typically opaque at the surface. The range of PWV that was experienced in the two campaigns provides a wealth of data that will be used to evaluate the water vapor spectroscopic parameters and continuum. The range of surface temperature at the two sites (RHUBC I surface temperatures ranged from –35° to –20°C, whereas the surface temperatures were between –10° and 5°C at Cerro

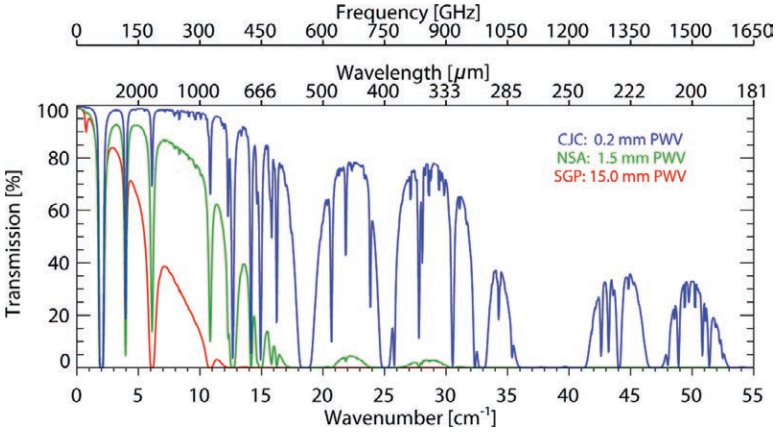

Fig. 7. The transmission in the submillimeter portion of the spectrum for the three atmospheres used in Fig. 1; the spectral resolution is 0.1 cm^{-1} (3 GHz). Strong oxygen absorption lines are located at 2.0, 3.9, 12.3, and 25.8 cm^{-1} (60, 118, 369, and 774 GHz, respectively).

Toco) should allow the temperature dependence of these parameters to be investigated. Changing just the water vapor absorption line parameters by using two different absorption line databases modified the global mean atmospheric absorption of solar radiation by about 3.5 (5.5) W m^{-2} in all-sky (clear sky) conditions, which did have a small impact on the hydrological cycle, cloud cover, and precipitation in a global climate model (Lohmann and Bennartz 2002); modifications of the water vapor continuum, which would effect a larger spectral range, may also have an appreciable impact. The datasets collected during these two experiments should lead to improved radiative transfer models in the strong water vapor absorption bands along with significantly smaller uncertainties, thereby improving an important component in global circulation models.

The RHUBC experiments have a second scientific objective for the far-infrared beyond water vapor spectroscopy. The imaginary refractive index of ice, and hence the absorption coefficient, has a minimum at 25 μm, which is significantly lower than the values in the 8–13-μm window (Warren 1984; see our Fig. 8). This implies that scattering by atmospheric ice particles is more important in the far-infrared relative to the mid-infrared, allowing more information on cirrus clouds to be obtained when using observation from both regions (Yang et al. 2003; Harries et al. 2008). Accurate cloud retrievals require that the single-scattering properties used in the retrievals are correct; however, because of the lack of spectrally resolved radiance observations in the far-infrared, the theoretical scattering properties in this band (e.g., Yang et al. 2003) have not been validated with atmospheric observations.

Data collected at the ARM NSA site, both during RHUBC I and at other times after the G-band water vapor radiometer (GVR) was deployed in 2007, can be used to evaluate ice crystal scattering properties for Arctic clouds. However, the properties of ice clouds change significantly from the poles to the tropics, and thus the results derived from the NSA site may not extend to other latitudes. Furthermore, since the properties of ice clouds vary considerably, a large observational dataset is needed to properly evaluate the single-scattering properties and radiative transfer models in ice cloud cases. We are currently pursuing, together with our RHUBC collaborators and others, the possibility of additional RHUBC campaigns, both ground-based and airborne, that will greatly increase our likelihood of observing single-layer cirrus clouds with far-infrared spectrometers and other complementary instruments.

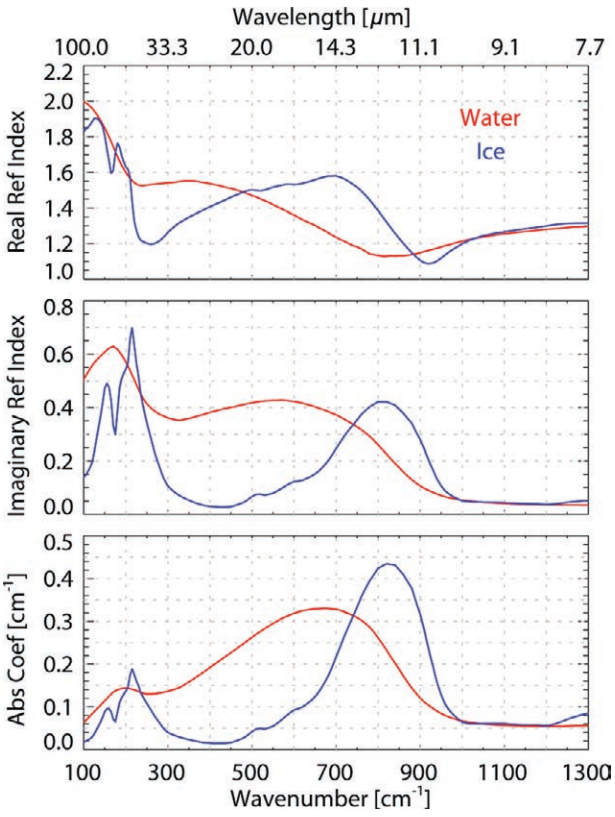

Fig. 8. The (top) real and (middle) imaginary refractive indices, and (bottom) the absorption coefficient, of liquid water (red) and ice (blue) in the mid- and far-infrared.

ACKNOWLEDGMENTS. The RHUBC campaigns were organized as part of the U.S. Department of Energy's Atmospheric Radiation Measurement (ARM) program, which is sponsored by the Office of Science, Office of Biological and Environmental Research, Climate and Environmental Sciences Division. RHUBC II was also supported in part by NASA, the Italian National Research Council, and the German Science Foundation (DFG). NASA participation in RHUBC II was made possible by support from the NASA Radiation Sciences Program (Dr. H. Haring, Program Manager) and the NASA Langley Research Center. We would like to thank all of the instrument PIs listed in Tables 1 and 2 (and their associates at their home institutions) for their help organizing and conducting these campaigns, as well as the ARM staff at Los Alamos National Laboratory, the ARM operators at the NSA site, and the technicians at AstroNorte in San Pedro for their efforts during these experiments. Analysis of RHUBC data is supported by ARM Grants DE-FG02-06ER64167, DE-FG02-90ER610, and DE-FG02-05ER64015, as well as the NASA ROSES proposal FORGE (Far-Infrared Observations of the Radiative Greenhouse Effect). Data collected during

these experiments are freely available via the ARM data archive at www.archive.arm.gov. Additional information on the RHUBC campaigns can be found at http://acrf-campaign.arm.gov/rhubc/.

REFERENCES

Ackerman, T. P. and G. M. Stokes, 2003: The Atmospheric Radiation Measurement program. *Phys. Today,* **56,** 38–44.

Bhawar, R., and Coauthors, 2008: Spectrally resolved observations of atmospheric emitted radiance in the H_2O rotation band. *Geophys. Res. Lett.,* **35,** L04812, doi:10.1029/2007GL032207.

Cady-Pereira, K. E., M. W. Shephard, D. D. Turner, E. J. Mlawer, S. A. Clough, and T. J. Wagner, 2008: Improved daytime column-integrated precipitable water vapor from Vaisala radiosonde humidity sensors. *J. Atmos. Oceanic Technol.,* **25,** 873–883.

Campbell, J. R., D. L. Hlavka, E. J. Welton, C. J. Flynn, D. D. Turner, J. D. Spinhirne, V. S. Scott, and I. H. Hwang, 2002: Full-time, eye-safe cloud and aerosol lidar observations at Atmospheric Radiation Measurement program sites: Instruments and data processing. *J. Atmos. Oceanic Technol.,* **19,** 431–442.

Canas, A. A., J. E. Murray, and J. E. Harries, 1997: The Tropospheric Airborne Fourier Transform Spectrometer. *Satellite Remote Sensing of Clouds and the Atmosphere II*, Joanna D. Haigh, Ed., International Society for Optical Engineering (SPIE Proceedings, Vol. 3220), 91–102.

Cimini, D., E. R. Westwater, A. J. Gasiewski, M. Klein, Y. V. Leuski, and S. G. Dowlatshahi, 2007: The ground-based scanning radiometer: A powerful tool for study of the Arctic atmosphere. *IEEE Trans. Geosci. Remote Sens.,* **45,** 2759–2777, doi:10.1109/TGRS.2007.897423.

——, F. Nasir, E. R. Westwater, V. H. Payne, D. D. Turner, E. J. Mlawer, M. L. Exner, and M. Cadeddu, 2009: Comparison of ground-based millimeter-wave observations and simulations in the Arctic winter. *IEEE Trans. Geosci. Remote Sens.,* **47,** 3098–3106, doi:10.1109/TGRS.2009.2020743.

Clough, S. A., and M. J. Iacono, 1995: Line-by-line calculations of atmospheric fluxes and cooling rates. 2. Application to carbon dioxide, ozone, methane, nitrous oxide and the halocarbons. *J. Geophys. Res.,* **100,** 162519–162535.

——, Y. Beers, J. P. Klein, and L. S. Rothman, 1973: Dipole moment of water from Stark measurements of H_2O, HDO, and D_2O. *J. Chem. Phys.,* **59,** 2254–2259.

——, F. X. Kneizys, and R. W. Davies, 1989: Line shape and the water vapor continuum. *Atmos. Res.,* **23,** 229–241.

——, M. J. Iacono, and J.-L. Moncet, 1992: Line-by-line calculations of atmospheric fluxes and cooling rates: Application to water vapor. *J. Geophys. Res.,* **97,** 15 761–15 785.

Crewell, S., and U. Löhnert, 2007: Accuracy of boundary layer temperature profiles retrieved with multifrequency multiangle microwave radiometery. *IEEE Trans. Geosci. Remote Sens.,* **45,** 2195–2201, doi:10.1109/TGRS.2006.888434.

Delamere, J. S., S. A. Clough, V. Payne, E. J. Mlawer, D. D. Turner, and R. Gamache, 2010: A far-infrared radiative closure study in the Arctic: Application to water vapor. *J. Geophys. Res.,* in press.

Evans, K. F., A. H. Evans, I. G. Nolt, and B. T. Marshall, 1999: The prospect for remote sensing of cirrus clouds with a submillimeter-wave spectrometer. *J. Appl. Meteor.,* **38,** 514–525.

Gettelman, A., P. M. de F. Forester, M. Fujiwara, Q. Fu, H. Vömel, L. K. Gohar, C. Johanson, and M. Ammerman, 2004: Radiation balance of the tropical tropopause layer. *J. Geophys. Res.,* **109,** D07103, doi:10.1029/2003JD004190.

Harries, J., and Coauthors, 2008: The far-infrared Earth. *Rev. Geophys.,* **46,** RG4004, doi:10.1029/2007RG000233.

Hawat, T., T. Stephen, and F. Murcray, 2002: Absolute solar transmittance interferometer for ground-based measurements. *Appl. Opt.,* **41,** 3582–3589.

Knuteson, R. O., and Coauthors, 2004a: The Atmospheric Emitted Radiance Interferometer. Part I: Instrument design. *J. Atmos. Oceanic Technol.,* **21,** 1763–1776.

——, and Coauthors, 2004b: The Atmospheric Emitted Radiance Interferometer. Part II: Instrument performance. *J. Atmos. Oceanic Technol.,* **21,** 1777–1789.

Lohmann, U., and R. Bennartz, 2002: Impact of improved near-infrared water vapor line data in simulations with the ECHAM4 general circulation model. *J. Geophys. Res.,* **107,** 4288, doi:10.1029/2001JD001101.

Miloshevich, L. M., H. Vömel, D. N. Whiteman, and T. Leblanc, 2009: Accuracy assessment and correction of Vaisala RS92 radiosonde water vapor measurements. *J. Geophys. Res.,* **114,** D11305, doi:10.1029/2008JD011565.

Mlawer, E. J., J. Traubman, P. D. Brown, M. J. Iacono, and S. A. Clough, 1997: RRTM, a validated correlated-*k* model for the longwave. *J. Geophys. Res.,* **102,** 16 663–16 682.

Mlynczak, M. G., and Coauthors, 2006: First light from the Far-Infrared Spectroscopy of the Troposphere

(FIRST) instrument. *Geophys. Res. Lett.,* **33,** L07704, doi:10.1029/2005GL025114.

Paine, S., R. Blundell, D. C. Papa, J. W. Barrett, and S. J. E. Radford, 2000: A Fourier transform spectrometer for measurement of atmospheric transmission at submillimeter wavelengths. *Publ. Astron. Soc. Pacific,* **112,** 108–118.

Palchetti, L., and Coauthors, 2005: Breadboard of the Fourier transform spectrometer for the Radiation Explorer in the Far Infrared (REFIR) atmospheric mission. *Appl. Opt.,* **44,** 2870–2878.

——, G. Bianchini, B. Carli, U. Cortesi, and S. Del Bianco, 2008: Measurement of the water vapor vertical profile and of the Earth's outgoing far infrared flux. *Atmos. Chem. Phys.,* **8,** 2885–2894.

Payne, V. H., J. S. Delamere, K. E. Cady-Pereira, R. R. Gamache, J.-L. Moncet, E. J. Mlawer, and S. A. Clough, 2008: Air-broadened half-widths of the 22- and 183-GHz water-vapor lines. *IEEE Trans. Geosci. Remote Sens.,* **46,** 3601–3617, doi:10.1109/TGRS.2008.2002435.

Pazmany, A. L, 2007: A compact 183-GHz radiometer for water vapor and liquid water sensing. *IEEE Trans. Geosci. Remote Sens.,* **45,** 2202–2206, doi:10.1109/TGRS.2006.888104.

Racette, P., and Coauthors, 2005: Measurement of low amounts of precipitable water vapor using ground-based millimeterwave radiometry. *J. Atmos. Oceanic Technol.,* **22,** 317–337.

Revercomb, H. E., and Coauthors, 2003: The ARM Program's water vapor intensive observation periods: Overview, initial accomplishments, and future challenges. *Bull. Amer. Meteor. Soc.,* **84,** 217–236.

Rose, T., S. Crewell, U. Löhnert, and C. Simmer, 2005: A network suitable microwave radiometer for operational monitoring of the cloudy atmosphere. *Atmos. Res.,* **75,** 183–200, doi:10.1016/j.atmosres.2004.12.005.

Rothman, L. S., and Coauthors, 2009: The HITRAN 2008 molecular spectroscopic database. *J. Quant. Spectrosc. Radiat. Trans.,* **110,** 533–572, doi:10.1016/j.jqsrt.2009.02.013.

Rutllant Costa, J., 1977: On the extreme aridity of coastal and Atacama deserts in northern Chile. Ph.D. dissertation, University of Wisconsin—Madison, 175 pp.

Stokes, G. M., and S. E. Schwartz, 1994: The Atmospheric Radiation Measurement (ARM) program: Programmatic background and design of the cloud and radiation test bed. *Bull. Amer. Meteor. Soc.,* **75,** 1201–1221.

Tobin, D. C., 1996: Infrared spectral lineshapes of water vapor and carbon dioxide. Ph.D. dissertation, University of Maryland, Baltimore County, 320 pp.

——, and Coauthors, 1999: Downwelling spectral radiance observations at the SHEBA ice station: Water vapor continuum measurements from 17-26 micrometers. *J. Geophys. Res.,* **104,** 2081–2092.

Turner, D. D., B. M. Lesht, S. A. Clough, J. C. Liljegren, H. E. Revercomb, and D. C. Tobin, 2003: Dry bias and variability in Vaisala RS80-H radiosondes: The ARM experience. *J. Atmos. Oceanic Technol.,* **20,** 117–132.

——, and Coauthors, 2004: The QME AERI LBLRTM: A closure experiment for downwelling high spectral resolution infrared radiance. *J. Atmos. Sci.,* **61,** 2657–2675.

——, M. Cadeddu, U. Lohnert, S. Crewell, and A. Vogelmann, 2009: Modifications to the water vapor continuum in the microwave suggested by ground-based 150-GHz observations. *IEEE Trans. Geosci. Remote Sens.,* **47,** 3326–3337, doi:10.1109/TGRS.2009.2022262.

Warren, S. G., 1984: Optical constants of ice from the ultraviolet to the microwave. *Appl. Opt.*, **23,** 1206–1225, doi:10.1364/AO.23.001206.

Yang, P., and Coauthors, 2003: Spectral signature of ice clouds in the far-infrared region: Single-scattering calculations and radiative sensitivity study. *J. Geophys. Res.,* **108,** D18, 4569, doi:10.1029/2002JD003291.